RR 18/92

THE BEHAVIOUR OF CEMENTED BACKFILL AND THE SURROUNDING ROCKMASS AT WESTERN DEEP LEVELS SOUTH MINE

G YORK AND A P SQUELCH
Rock Engineering

REFERENCE REPORT NO. 18/92
PROJECT NO. GR1R
NOVEMBER 1992

KEYWORDS: CEMENTED BACKFILL
K RATIO
CONFINED COMPRESSION
CLOSURE
DILATION

PREFACE

As part of its work programme for the development and evaluation of backfill materials for regional and local support, COMRO has assessed the performance of a wide range of backfill both in the laboratory and underground in mines. Work on this evaluation programme effectively ceased during 1992 at the request of industry and this report documents the last of the backfill types to be quantitatively evaluated, namely cemented backfill. As with previous evaluation of the in situ performance of backfill, determination of the performance of cemented backfill has taken a long time, two years. The results, however, have been very encouraging. It has been shown that cemented backfill provides excellent local and regional support at high stoping widths at Western Deep Levels South Mine. In addition, quantitative measurements of the backfill behaviour under confined compression, together with information on the rock mass behaviour, have been obtained. This information will enable the design of better backfill materials, using non-linear modelling programs, for specific problem areas in mines.

N C GAY

SYNOPSIS

Cemented backfill is used at Western Deep Levels Mine as local and regional support in areas of high stoping width. The in situ performance is reported and compared to laboratory tests. A back analysis was carried out to obtain a more accurate value of the in situ (Young's) modulus for the elastic modelling computer program MINSIM-D. The in situ modulus was found to be in the range 45-50 GPa.

The in situ results show that the VCR hangingwall has significant closure components. Smaller dip spans (compared to other longwall applications) and the lack of bedding planes in the hangingwall result in lower backfill stresses needed to clamp the hangingwall. Laboratory and in situ results indicate that there is a distinct transition point between fully and partially confined compression due to dilation.

The use of cemented backfill in the high stoping widths at WDL South Mine has been successful in that shrinkage is negligible and dilation is minimised. Cemented backfill provides support much sooner, and is stiffer, than uncemented backfill. Backfill is superior to packs in that packs yield while backfill sustains increasing loads.

CONTENTS

LIST OF FIGURES

1 INTRODUCTION

Research into cemented backfill has been confined to three areas. The first area is applications of cemented rockfill for rockburst control. Quesnel et al. (1989) reported a reduction in rockburst frequency, and where a burst occurred, a reduction in damage as compared to unconsolidated waste development rock backfills.

The second area has been computer modelling and laboratory testing of cemented backfill materials (Whyatt et al., 1989 and Lamos and Clarke, 1989), while a third area has been the investigations into alternative binding agents for backfill (Hopkins and Beaudry, 1989; Viles et al., 1989).

The stoping widths in the VCR reef at Western Deep Levels South Mine were as high as four metres. Uncemented backfill would slump and shrink excessively in such high stoping widths. Cemented backfill was employed to counter the effects of a high stoping width, by providing a higher initial stiffness and better hangingwall contact.

A long term monitoring and measurement programme to fully quantify the in situ performance of cemented backfill has yet to be reported. This report documents a monitoring programme on cemented backfill at Western Deep Levels South Mine which has enabled the complete backfill rib (bag) behaviour and confined compression behaviour to be assessed. The monitoring programme took place at three installations over a period of almost two years.

Laboratory simulations of the in situ installations were also performed. These results and how they relate to in situ measurements are reported. Theoretical elastic closures were determined (using MINSIM-D) and are compared to in situ closures, both absolute values and rates of closure.

2 IN SITU MEASUREMENTS

2.1 Backfill Material

The backfill composition is a mixture of classified tailings backfill from the WDL mine, Ordinary Portland Cement (OPC) and a commercially available binder. The mixture is pumped at a relative density (RD) of approximately 1,7. The cement content as a percentage of the total mass of the slurry was approximately six per cent (or approximately 15 per cent of the total dry mass), while the accelerator content was approximately 0,5 per cent.

2.2 Description of Sites

The cemented backfill sites are at Western Deep Levels South Mine, in the 80/49 E3 panel (Figure 1). The average depth is 2150 m , with a variable dip of 10-15°. Three installations (A,B and C) were placed sequentially with face advance. Installation B is 10 m closer to the face than installation A, while installation C is 49 m closer to the face.

Each installation consisted of three stations inside the bag and one closure ride station outside the bag on the up dip side, except installation C at which simple closures were measured up dip of the bag. Each station inside the bag consisted of a triaxial stress cell with a mechanical closure meter. The triaxial stress cell is able to measure stresses in the vertical, dip and strike directions, while the mechanical closure meter enables strains to be calculated for each station.

The triaxial cells were installed to measure the confined compression behaviour of the cemented backfill, while the three installations inside the bags and the one

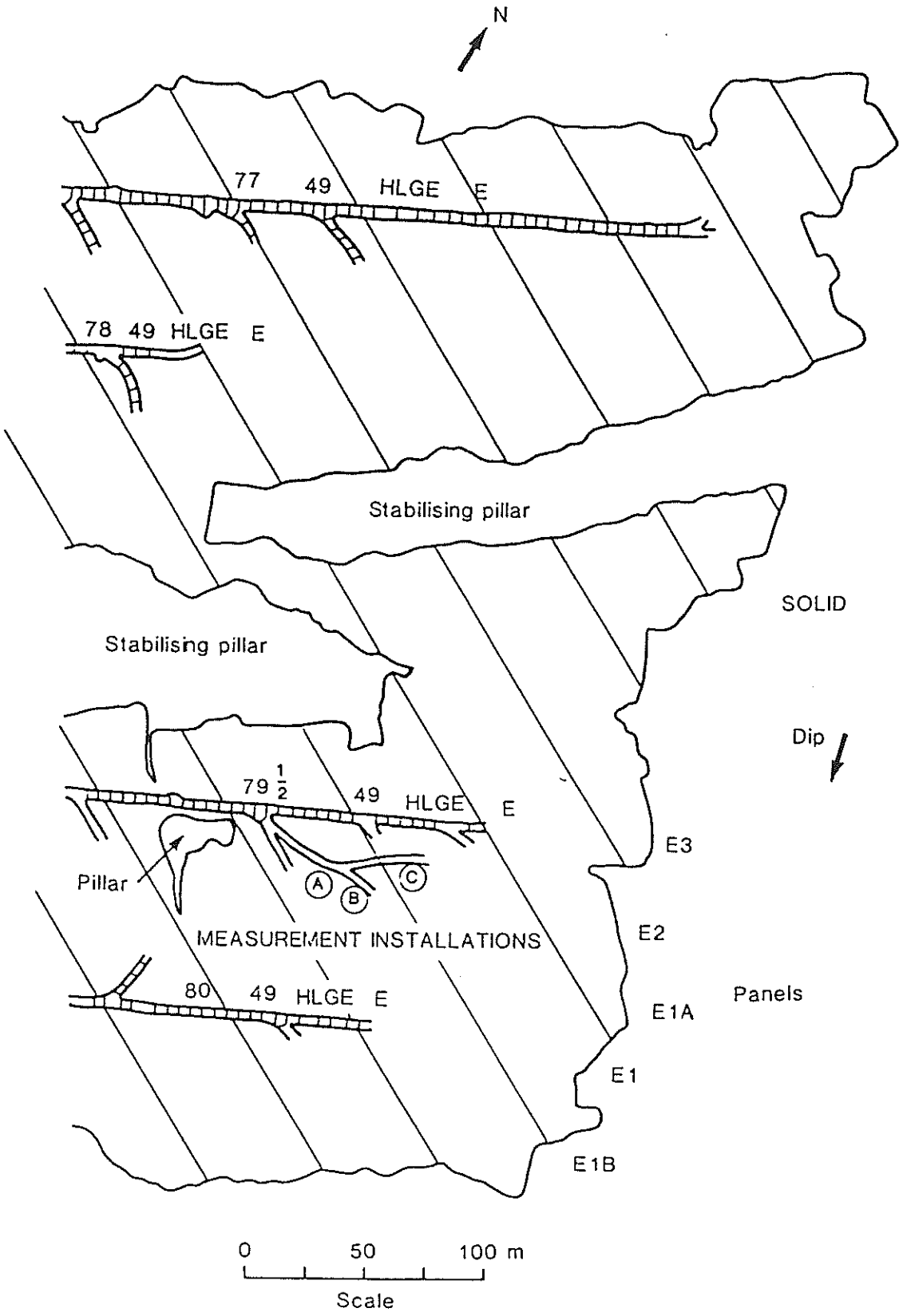

Fig. 1 - Plan showing general position of measurement installations A, B and C at Western Deep Levels South Mine

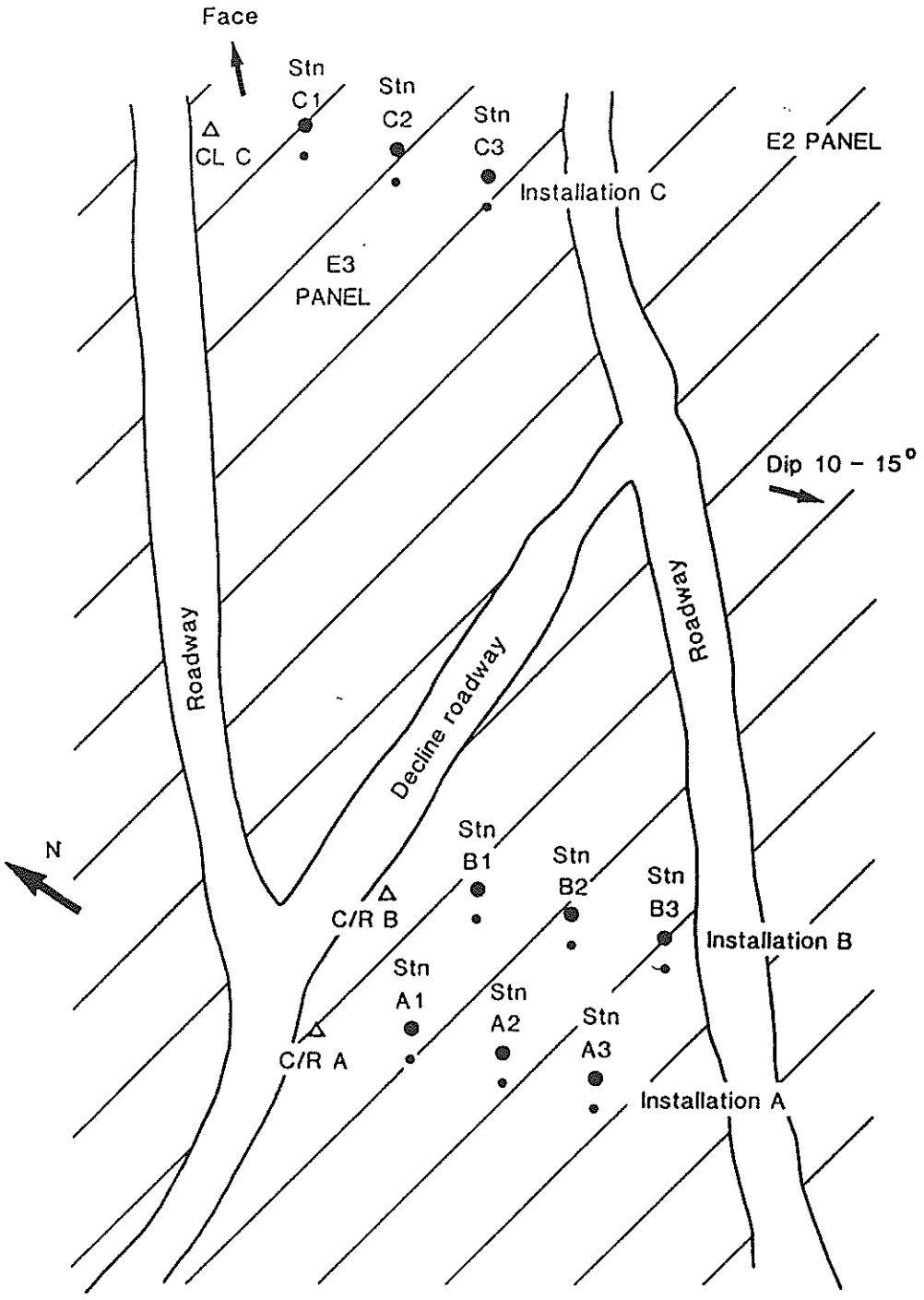

Fig. 2 - Plan of measurement installations showing relative positions of triaxial stress meter cells and closure installations

closure ride station outside the bags was intended to supply data for an assessment of the complete backfill rib behaviour.

The stoping widths decreased with face advance. The stoping widths at installations A, B and C were 3,82 m, 3,61 m and 2,34 m respectively.

2.3 Results

2.3.1 Confined Compression/Stress-Strain Behaviour

Gürtunca et al. (1989) and Squelch (1990) have shown that partial confinement conditions exist at the edge of a backfill bag due to dilation, and that the extent of the partial confinement down dip from the edge of the bag may be two to three metres from the edge of the backfill. Stations 2 and 3 at each installation are considered to be fully confined in the dip and strike direction because they are positioned at least 8,5 m down dip from the edge of the backfill bag.

The results of the confined compression behaviour for station 2 at installation A are shown in Figure 3. The graph shows that strain at a vertical stress of approximately 2,6 MPa was approximately 5 per cent. Similar results were obtained at station 1 of installation B (Figure 4). The results for the other stations are not shown because

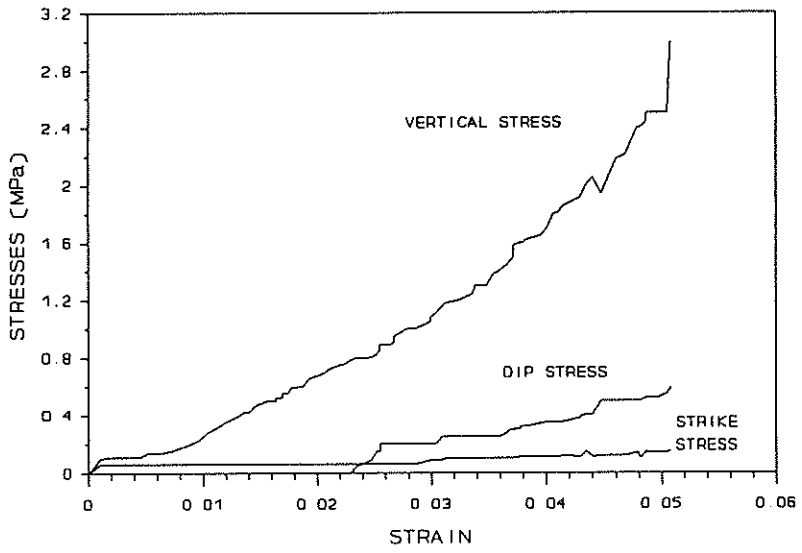

Fig. 3 - Confined compression behaviour at station A2

they are qualitatively the same. These results are shown in APPENDIX I.

Of particular interest are the determination of the K ratios in the backfill (K ratio is defined as the ratio of horizontal stress to vertical stress). A constant or almost constant K ratio is defined as the Ko ratio. Once a Ko ratio has been attained, any vertical stress increase is then matched by a proportionate increase in horizontal stress, depending on the value of Ko. A dip and a strike K ratio were calculated for each station. The results for installation A, B and C are shown in Figures 5-7. The K ratio is of interest when considering the confined compression behaviour of the cemented backfill.

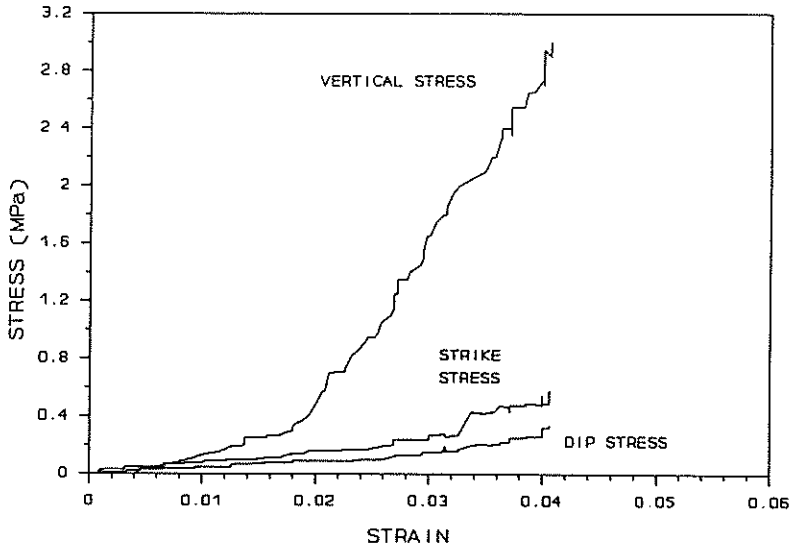

Fig. 4 - Stress strain behaviour at station B1

The range of Ko was 0,03 to 0,44. A low Ko ratio is produced by a low horizontal stress. The very low Ko ratios were due to stress meters that were not functioning correctly. This will be discussed further in the report.

2.3.2 Complete Backfill Rib Behaviour

Results of relevance to the complete backfill rib behaviour were determined from the closure profiles, dip closure profiles and dip stress profiles. The closure profiles for installations A and B are shown in Figures 8 and 9.

The closure meter at station C2 never worked satisfactorily, while the closure meter at station C3 ceased operating fairly soon after installation. Initially, the closure increments for station C1 were used for stations C2 and C3. After the hanging wall over the gully and the bag was closing at the same rate, the closure increments from the closure station outside the bag were used for the closures inside the bag.

The detailed closure profiles and dip profiles will thus not be shown for installation C and neither will they be used in the discussion. Installation C is nevertheless useful to provide a general indication of strains and as an aid in discussion. The stress measurements are regarded as accurate.

The closure meters inside the bags seem to have ceased operating because the stresses increase, with little corresponding increase in closure. It is possible that the backfill may be getting stiffer, but the stresses and strains are at this stage too low for the strains to start showing an asymptotic trend.

Figures 10 and 11 show the dip closure profiles for installations A and B. Each line represents closures at any one time along the dip section. The time gap between each line is approximately one month, except where the lines would have been too close to each other to produce a clear figure. The stresses at each point are shown, as are the distances to the face.

Dip stress profiles show the stress distribution along a dip section of the bag for a given strain. These stresses will have occurred at different times. The effect of

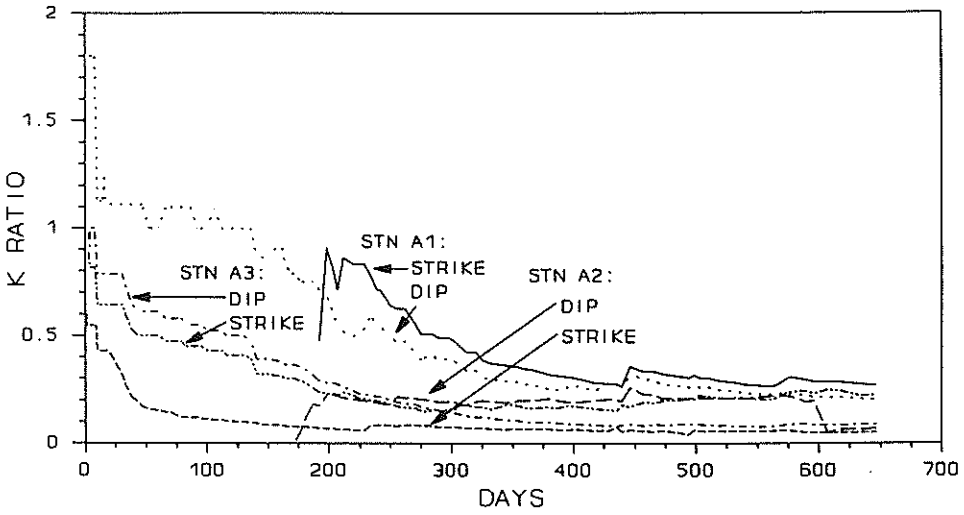

Fig. 5 - K ratios for installation A

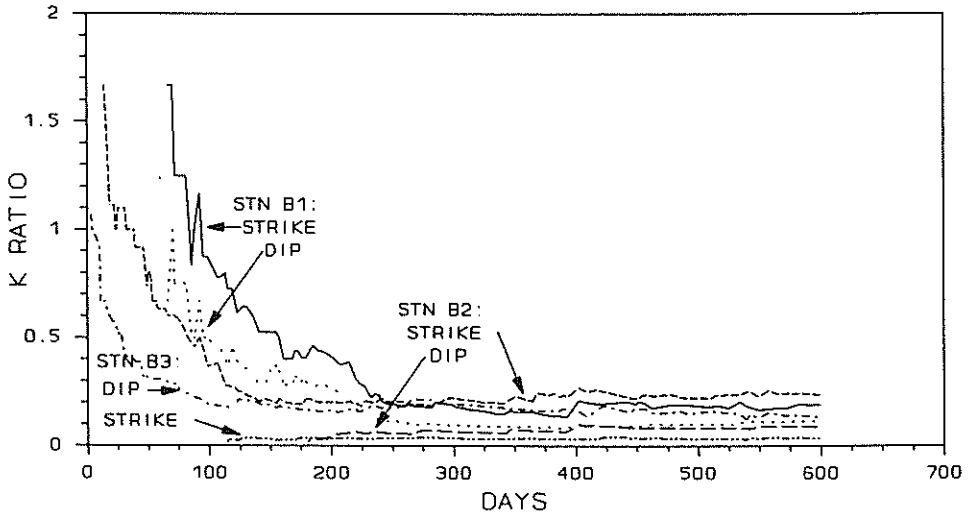

Fig. 6 - K ratios for installation B

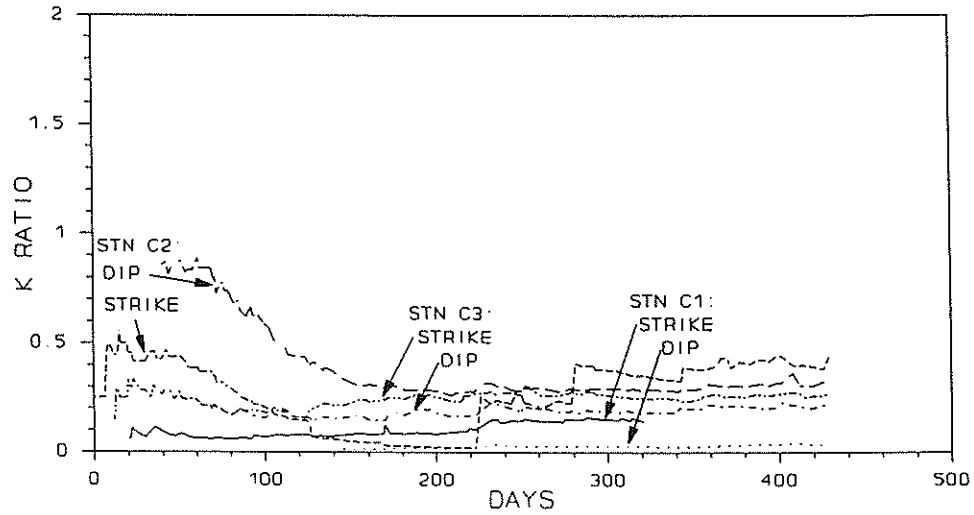

Fig. 7 - K ratios for installation C

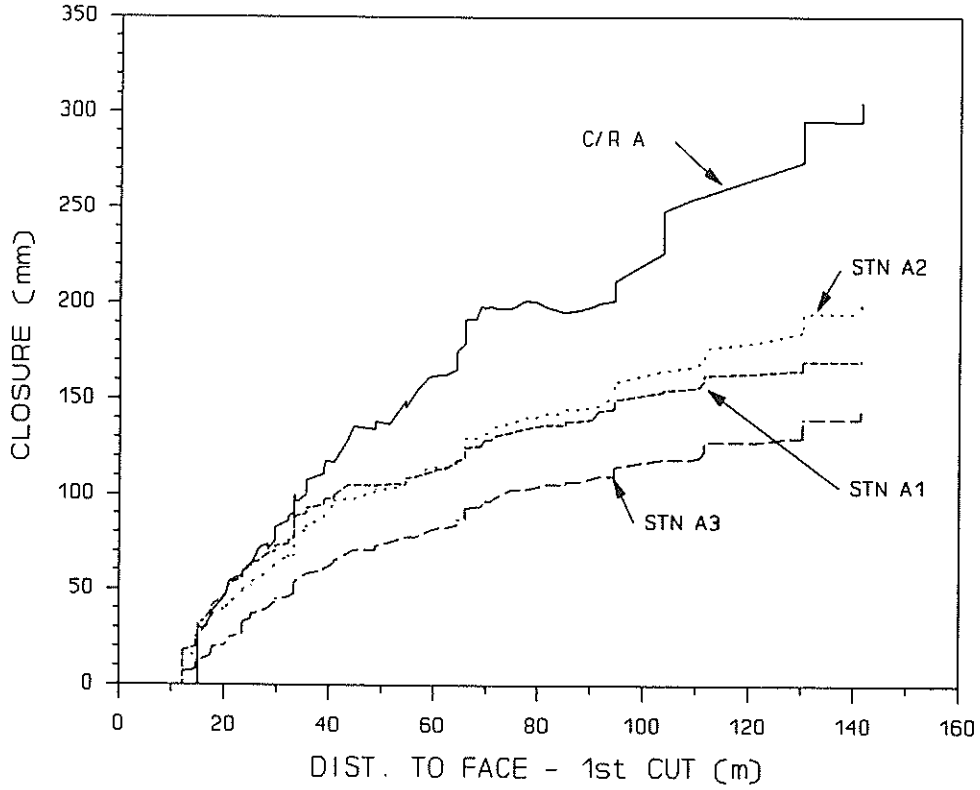

Fig. 8 - Closure profile for installation A

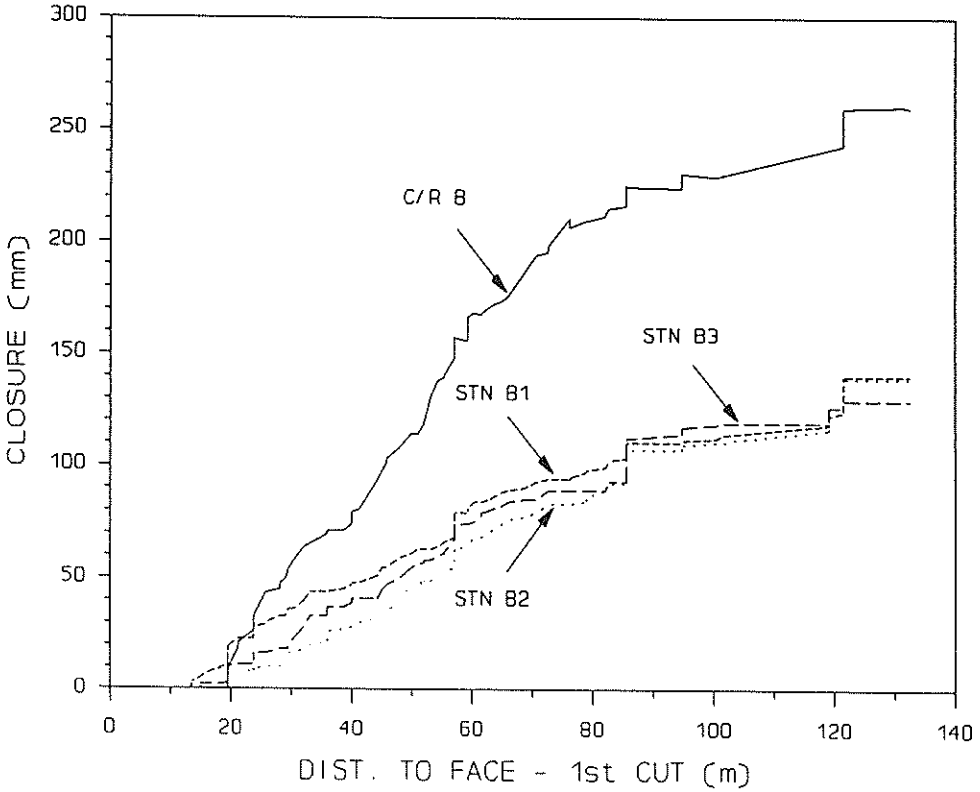

Fig. 9 - Closure profile for installation B

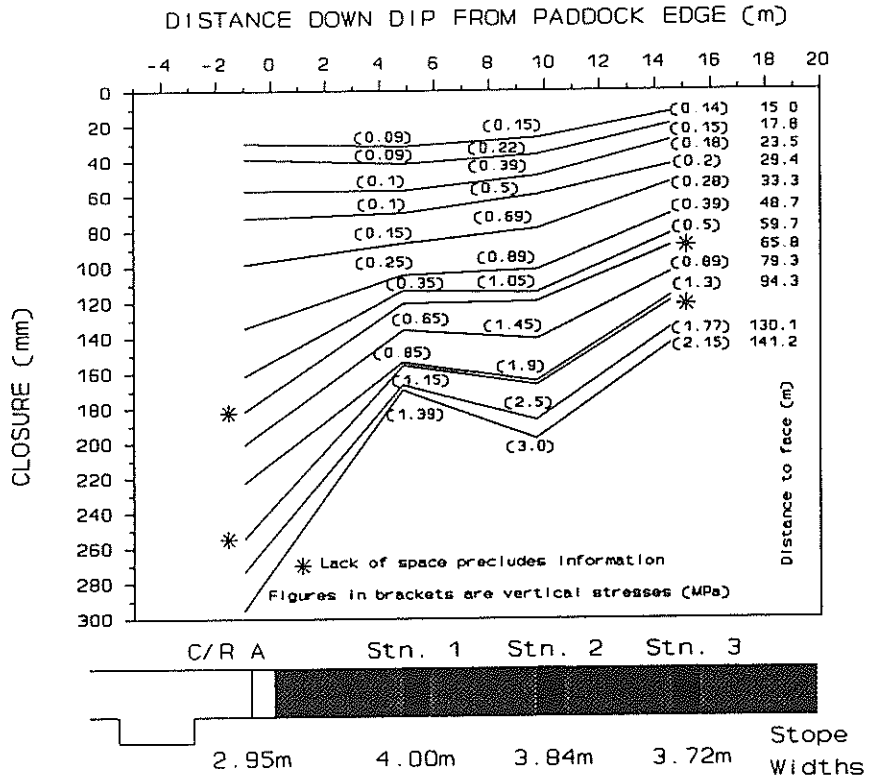

Fig. 10 - Dip closure profile for installation A

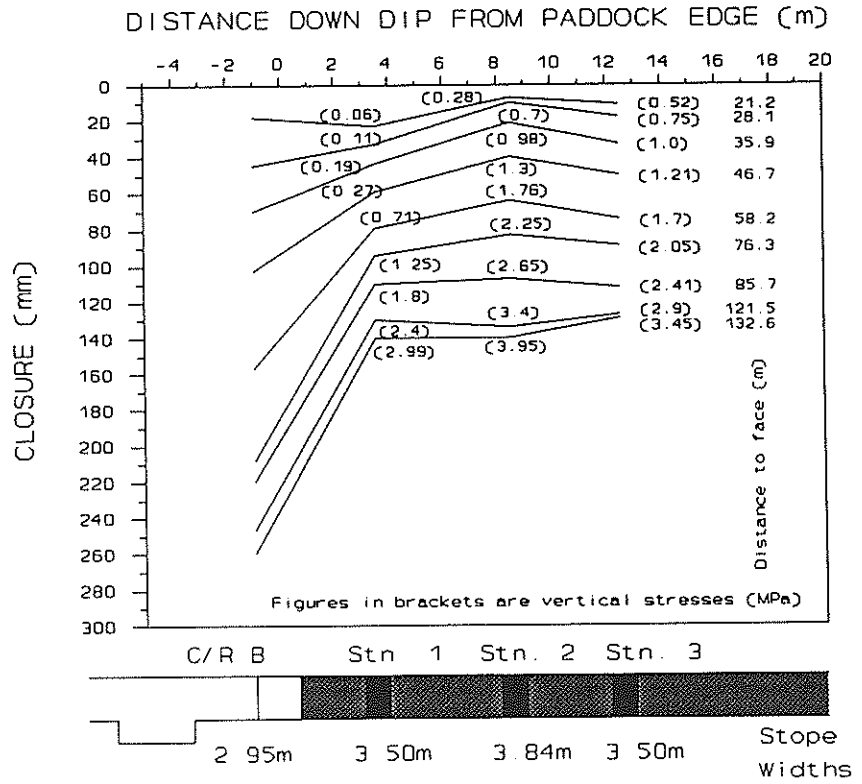

Fig. 11 - Dip closure profile for installation B

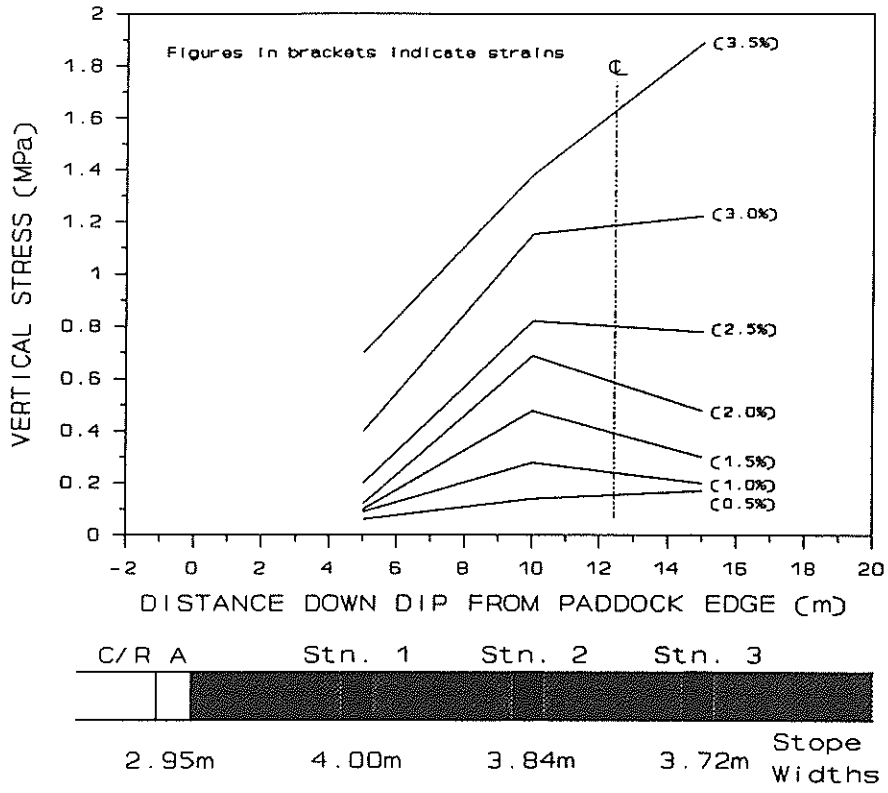

Fig 12 - Dip stress profile for installation A

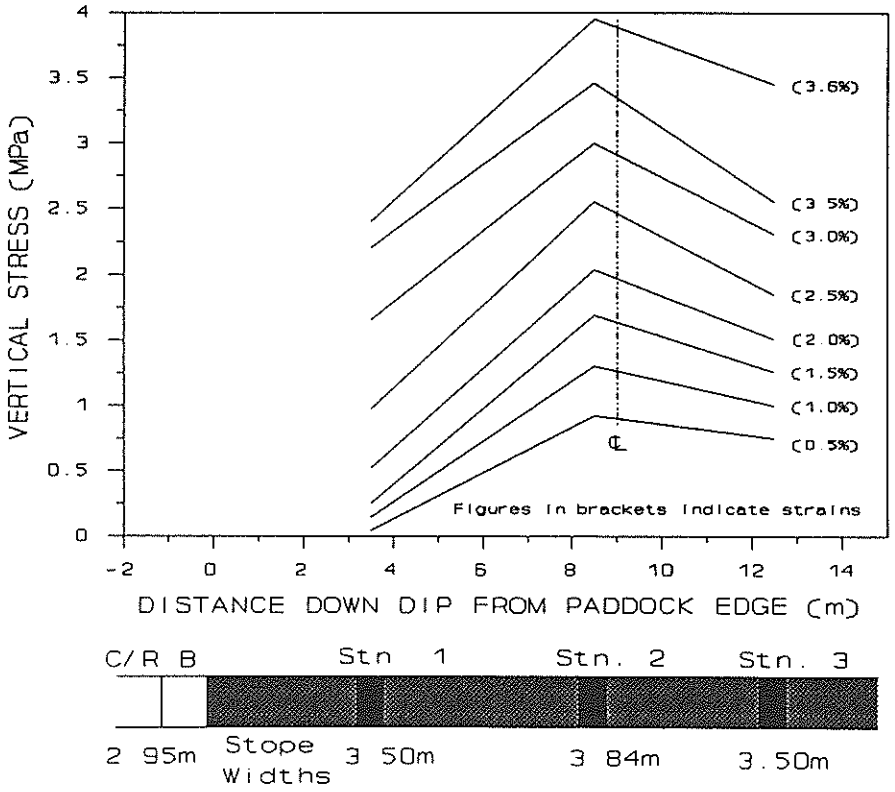

Fig 13 - Dip stress profile for installation B

varying stope width is to some extent nullified by plotting stress contours at equal strains rather than equal closures. The plots of dip stress profiles for installations A and B are shown in Figures 12 and 13.

3 LABORATORY TESTS

The in situ results showed K ratios of low values (in the range 0,03 to 0,44) when compared to other types of backfill. Gürtunca and Adams (1991) plotted Ko values in the range 0,3 to 0,5 for dewatered tailings and classified tailings backfill. Adams et al. (1991) have reported Ko ratio values in a band between 0,3 and 0,6 for comminuted waste backfill. While it was recognised that the strain values were relatively low, it was decided to perform a large scale laboratory test to confirm the in situ results and to further investigate the properties of cemented backfill. Two tests were performed. The first test was unconfined while the second test was fully confined in one horizontal direction and semi-confined in the other horizontal direction.

3.1 Material

The backfill material used for the laboratory tests approximated closely to that of the in situ backfill. The materials were obtained from Western Deep Levels South Mine. The constituents were classified tailings, OPC and a commercially available accelerator. The mix ratio was five per cent OPC and one per cent accelerator.

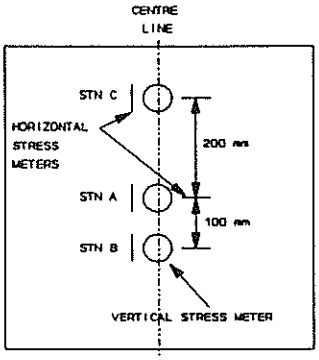

Fig. 14 - Plan view of laboratory test 1

3.2 Test 1-Unconfined

The first laboratory test was performed on a completely unconfined specimen of size 600x600 mm by 315 mm high. The sample was cured for 35 days. Triaxial stress meter cells were placed as shown in Figure 14. The sample was loaded at a constant strain rate until a vertical stress of 10 MPa was reached in the centre of the backfill.

3.2.1 Results

The sample edges showed significant spalling as it was compressed, with large chunks of material breaking away completely. As a result of this, only station A at the centre of the sample recorded any significant stress increase. Figure 15 shows the results for the vertical stress at each of the three stations. One of the horizontal stress meters at station A did not work. The final K ratios for station A ranged from 0,3 to 0,46. The K ratio at the highest stress (10 MPa) was 0,32.

There was a stress drop at 2,5 MPa vertical stress and a subsequent stress build up. This behaviour was qualitatively observed by Lamos and Clarke (1989) for unconfined cemented backfill.

A number of adjustments were made to the test in the light of the results. Confined compression conditions exist in situ in the strike direction, while the dip direction is, as will later be shown, well confined. The in situ vertical to horizontal aspect ratio is approximately 1:6 to 1:7. The confined test described in the next section incorporated these corrections.

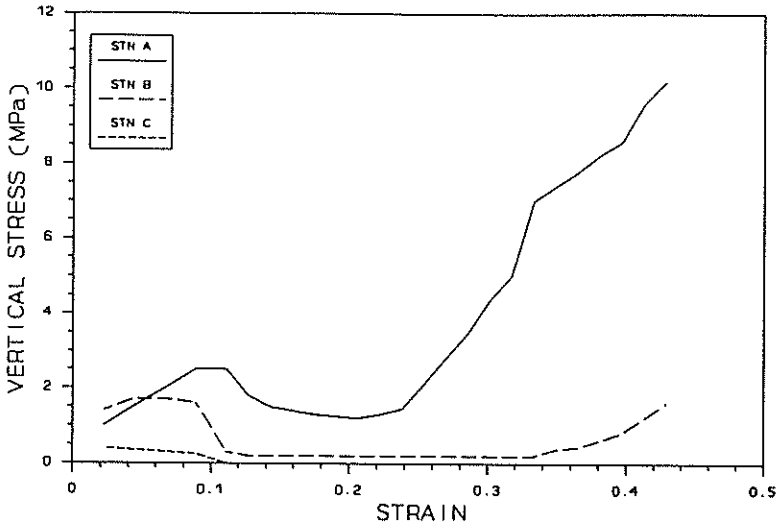

Fig. 15 - Vertical stress v strain for laboratory test 1-unconfined

3.3 Test 2-Confined

The second laboratory test was carried out to more accurately simulate in situ conditions. The best aspect ratio obtainable within practical limits was 1:5. The sample was 1000x1000 mm in plan and 200 mm deep, with four triaxial load cells as shown in Figure 16.

One horizontal direction was fully confined and thus corresponds to the in situ strike direction. The other horizontal direction was semi-confined by geotextile fabric similar to that used in situ. This corresponds to the in situ dip direction. Again, load was applied at a constant strain rate after a curing period of 35 days.

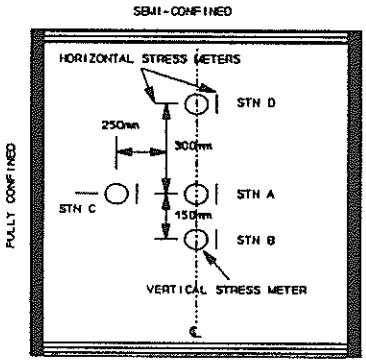

Fig. 16 - Plan view of laboratory test 2

3.3.1 Results

Figure 17 shows the vertical stress at each station plotted against strain. The maximum load applied was 17,15 MN, while the maximum stress measured was 33,25 MPa at station C. The corresponding stress at station A was 31,90 MPa. At this point the test was stopped because the testing machine had reached its maximum capacity. The vertical stress meter at station B burst after a stress of 4,2 MPa had been reached. The vertical stresses at stations B and C were identical until the stress meter at station B broke. The strains at any point in the specimen are equal at any one time. Hence, by referring to Figure 17, it can be seen that the curves for stations B and C are superimposed exactly until a stress of 4,2 MPa is reached.

Considerable dilation was observed at the two sides semi-confined by geotextile fabric. The final amount was 20 per cent, 10 per cent on each side.

The vertical stress at station D tapered off and fell away after reaching a maximum stress of 4,46 MPa. Station D was placed 200 mm from the edge of the sample.

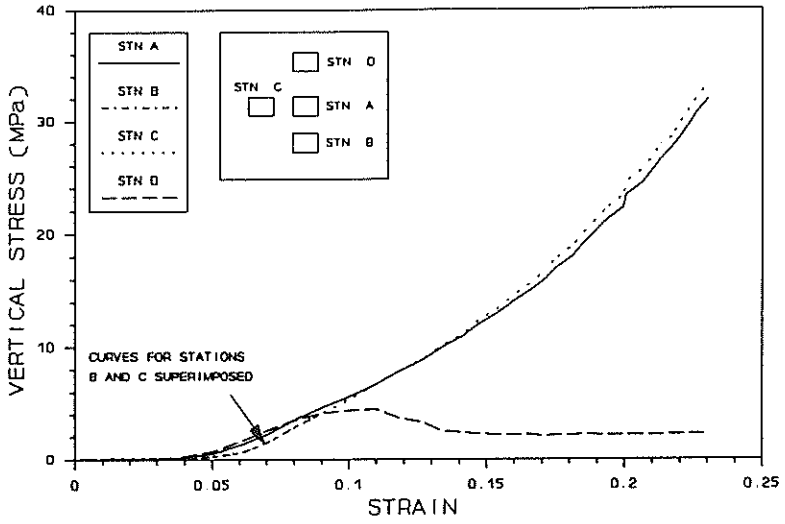

Fig. 17 - Vertical stress v strain for all four stations for laboratory test 2-confined

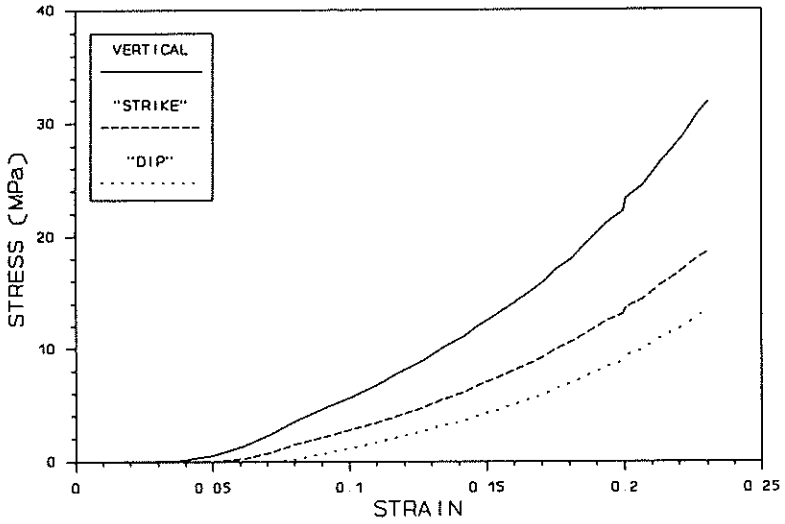

Fig. 18 - Confined compression behaviour for station A in laboratory test 2-confined

When the test was completed and the triaxial stress meter cells were excavated, it was noticed that there were two bands of relative softness. These bands were at the semi-confined edges of the sample. The region inside these bands was considerably harder. Station D was placed exactly in the transition zone between the soft and the hard regions.

It is clear that station A in the middle was fully confined. The stress strain curve, as shown in Figure 18, can thus be interpreted as confined compression behaviour.

The K ratio-strain graphs are presented in Figures 19 and 20. The two stations that were in the hard region, namely stations A and C, had final K ratios (i.e. Ko ratios) of 0,42 in the semi-confined dip direction (Figure 19). The Ko ratio for station C in the confined strike direction was 0,44 (Figure 20). These results are remarkable in their agreement. The Ko ratio for station A in the strike direction was 0,58, which

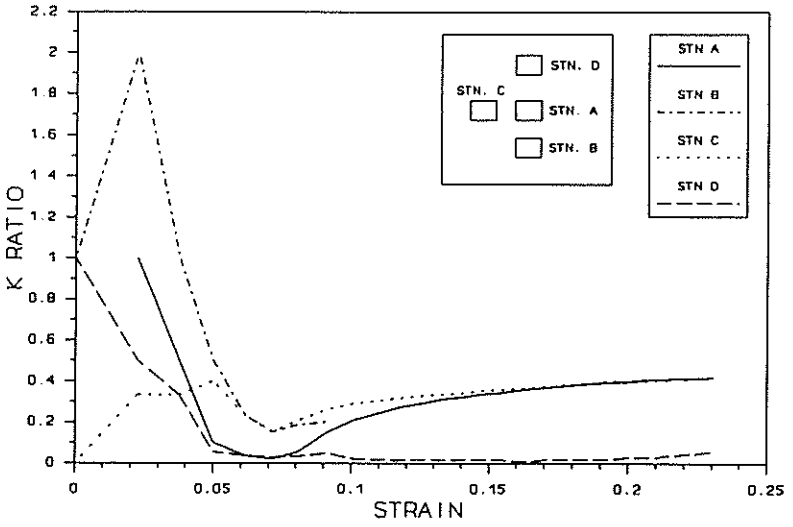

Fig. 19 - K ratios in the semi-confined direction for laboratory test 2

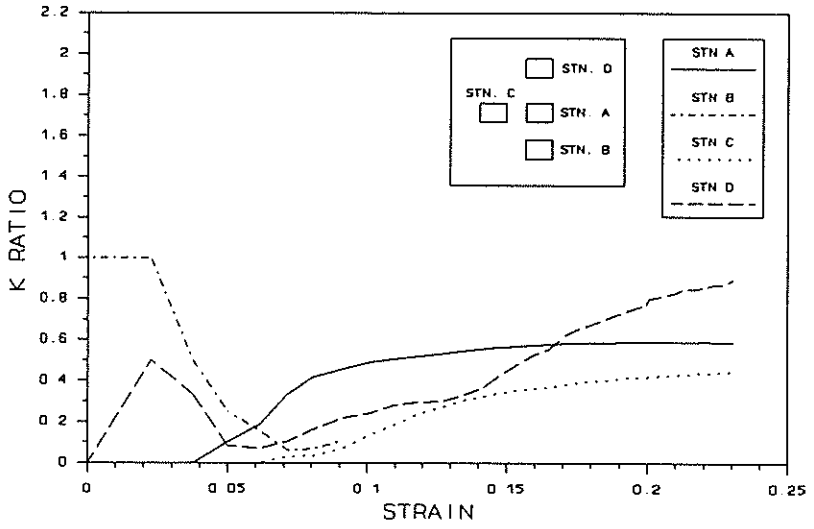

Fig. 20 - K ratios in the confined direction for laboratory test 2

is a reasonable variation.

From the figures it can be seen that the K ratios for station B (which was also in the hard region) show a similar trend to that of station C, until the vertical stress meter burst. The K ratios for station D are higher in the strike direction compared to those in the dip direction.

4 ELASTIC CLOSURE COMPARED TO IN SITU CLOSURE

The underground layout including the backfilled areas were modelled using MINSIM-D, a linear elastic computer model. The model used to simulate the backfill behaviour was the hyperbolic stress strain model. The values of a and b for the hyperbolic curve were based on the in situ results.

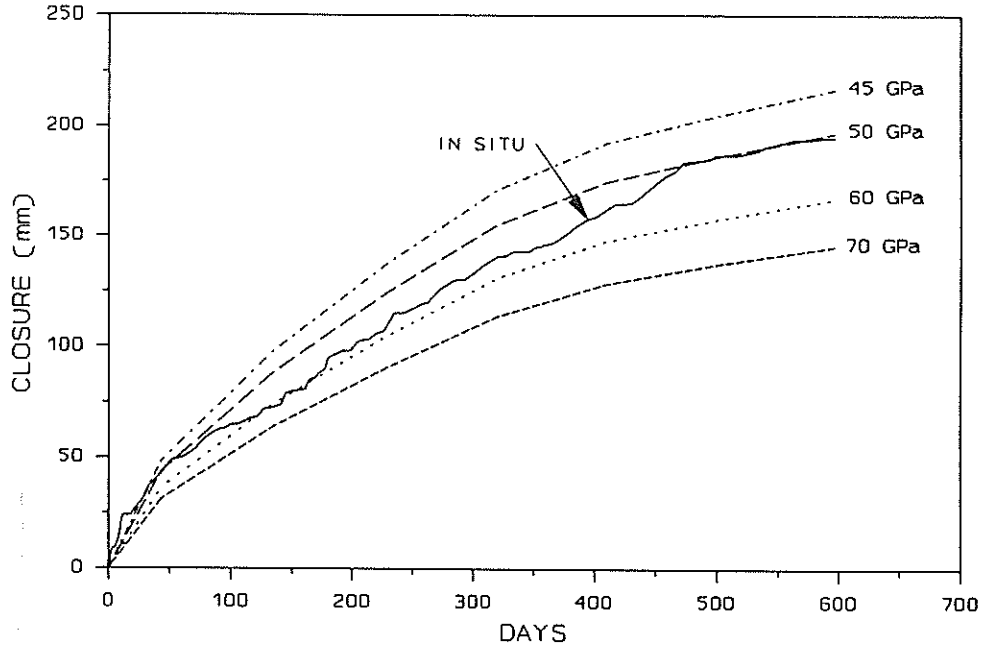

Fig. 21 - Plots of in situ closure and elastic closures (Minsim-D) for various values of in situ moduli for installation A

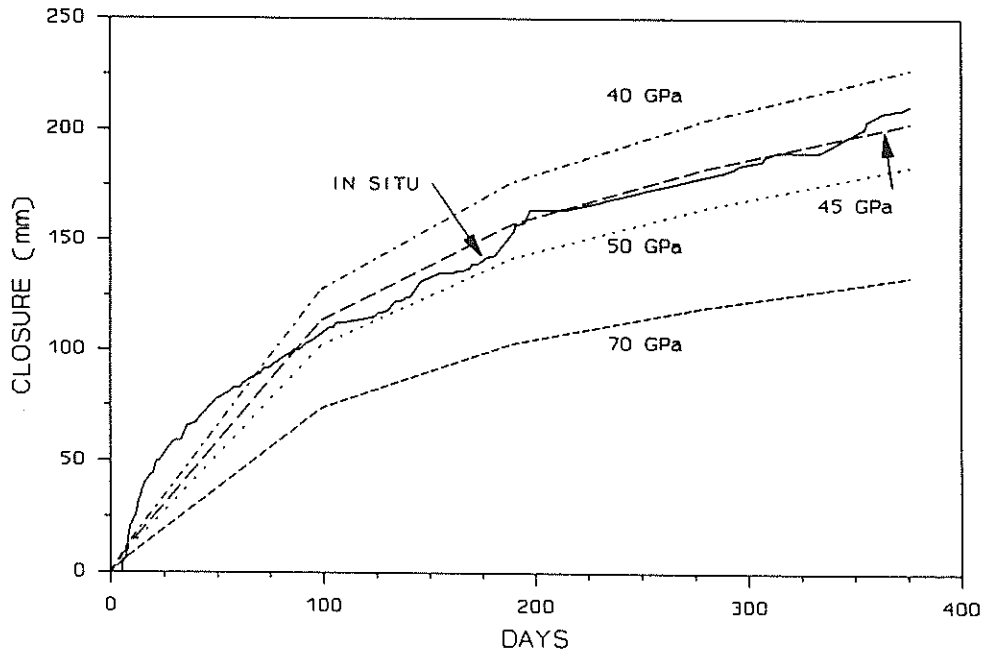

Fig. 22 - Plots of in situ closure and elastic closures (Minsim-D) for various values of in situ moduli for installation C

The in situ results from the central stations at installations A and C are shown in Figures 21 and 22. These curves are compared to various MINSIM-D closure profiles for different values of in situ (Young's) modulus. The profile for E=70 GPa is plotted as a reference line. These results will be discussed later.

Installation B was not used for this exercise, as will be discussed later.

5 DISCUSSION

5.1 In Situ Confined Compression Behaviour

Confined compression behaviour is assumed to take place near the centre of a bag. Figure 3 shows the increase in dip and strike stresses as vertical stress increases for station A2, which is near the centre of the bag.

It may be expected that large initial dilation of the backfill bag may be experienced due to the high stoping width and the slump of the cemented backfill before it has cured. The geotextile fabric and wire meshes both up and down dip of the bag and the packs down dip probably acted to provide some initial resistance to slump until the cemented backfill had developed enough stiffness (by curing) to support its own weight and thus prevent excessive initial dilation.

The K ratio-strain graphs give a good indication of confined compression behaviour. The K ratios start at values as high as 2, and then decrease progressively to stable values (Figures 5-7). Some stations achieve Ko conditions earlier than others.

The backfill at these stations shows banding of the strike and dip K ratios, to a lesser or greater degree. Banding in this context implies that the strike and dip K ratios for a station are similar to each other and form a distinct pair of lines on the graph. At installation A (Figure 5), the banding is evident over the entire monitoring period for stations A1 and A3, while the banding is not evident for station A2. At installation B (Figure 6), only station B1 shows banding. At installation C (Figure 7), station C3 shows tight banding over the entire monitoring period, while station C2 shows tight banding over the latter third of the monitoring period. Although station C1 forms a distinct pair, the values of dip and strike K ratio are not similar, and the dip K ratio is negligible.

Of the stations that have not been identified as exhibiting similar dip and strike K ratios, stations A2, B3 and C1 have either a dip or a strike K ratio less than 0,05. The other station not identified as banded, station B2, has a dip Ko ratio of 0,08. Of these stations, A2, B2 and B3 are in confined compression because of their position in the bag. The horizontal stress should therefore be a significant proportion of the vertical stress measured. Stress ratios less than 0,05 are therefore assumed to be due to malfunctioning horizontal stress meters. Disregarding these Ko values, the average Ko ratio then becomes 0,22, with a range of 0,09 to 0,44.

Tight banding implies a high degree of similarity between confinement conditions in the strike and dip directions. Of the nine stations, five clearly show very similar confinement conditions, while it is proposed that the other four stations that did not show similar conditions may have had malfunctioning stress meters. Of the five stations at which tight banding has been identified, four of them showed tight banding soon after measurements began, showing that loading conditions in the strike and dip directions were similar even before the cemented backfill had fully cured.

The backfill bag is not able to move or dilate in the strike direction due to bags already placed behind the bag and subsequent bags installed in front of the bag as mining progresses. The confinement conditions in the strike direction can thus be taken as fully confined. As stated above, the similar Ko ratios show that confinement conditions are the same in the strike and dip directions. It is thus clear that the dip direction is fully confined, with a transition point (Adams et al., 1991) between full and partial confinement near the edges of the backfill. This will be

discussed in more detail later in the next section. This also implies that there is little or no lateral movement in the dip direction (Adams et al., 1991).

The vertical stresses at which Ko conditions start range from 0,70 MPa to 1,58 MPa, with an average of just under 1 MPa. Thus, at a vertical stress of 1 MPa, most irregularities and interlocking particles that have the potential to slip or move have been consolidated and the cemented backfill behaves as an integral transversely isotropic medium. The consolidation process occurs over a long time period. The average time period was 225 days, ranging from 125 days to 430 days. Station C1 (Figure 7) was ignored for this calculation because there is no clear transition point between partial and full confinement conditions.

5.2 Complete Backfill Rib Behaviour

As mentioned previously, the closure profiles and dip closure profiles provide an indication of the overall backfill rib behaviour and its influence on the hangingwall.

It can be seen in Figure 8 that the closure ride station A and the bag closure meters close at similar rates until 65 mm of closure have occurred, at a distance to face of 25 m. The closure rate at station A3 is lower than those of stations A1 and A2. This will be discussed at the end of this section. Subsequently, the rate of closure in the gully (C/R A) increases at more or less the same rate as before, but the rates of closure inside the bag start to decrease. A differential closure rate thus develops, as shown by an increasing gap between the gully closure and the bag closures. The trend stops at a distance to face of 65,8 m. The closure lines for C/R A and the bag become approximately parallel, although there is still divergence.

Figure 10 confirms the above discussion. The lines are initially parallel, indicating similar rates of closure in the gully and the bag. The lines then diverge, corresponding to the differential closure rates mentioned. The lines then become parallel, corresponding to similar rates of closure in the gully and bag. The closure line for 65,8 m from the face is shown.

In installation A, the vertical stress at which differential closure began was less than 0,5 MPa, while the average vertical stress at which clamping started was 0,81 MPa.

Figures 9 and 11 show the closure and dip closure profiles for installation B. The trends discussed above are clearer in these figures. Differential closure starts at a distance to face of approximately 20 m at when the average stress is 0,32 MPa. Similar closure rates start at a distance to face of approximately 76,3 m at an average stress of 1,85 MPa.

This behaviour of similar closures followed by differential closures followed by similar closures was observed and explained by Gürtunca et al. (1989). The initial closures are similar over the gully and the bag because the stresses in the backfill are to low to provide resistance to the elastic and inelastic closures.

As closure increases and the backfill drains and cures, the stresses in the backfill start increasing. Although the stresses in the backfill are not high (less than 1 MPa in this case), the backfill begins to offer resistance to closure. At this time, the closure rates in the bag start decreasing while the closure rates in the gully continue at the higher rate, leading to the differential closure rates discussed above. During this time, inelastic movements are taking place, both over the gully and the bag.

The final phase is when sufficient work is being done by the backfill to generate enough vertical stress in the hangingwall to clamp the hangingwall into a single intact beam. The hangingwall over the bag and gully are forced to move downwards as a single intact structure. When this occurs, only elastic movement can take place.

The vertical stresses at which differential closure starts are given as 1 MPa and at which clamping starts as 3 to 4 MPa in the case of uncemented backfill (Gürtunca et al., 1989). Differential closure started at less than 0,5 MPa at the cemented backfill installations, while clamping started at less than 1 MPa at installation A and approximately 2 MPa at installation B.

The lower vertical stresses for cemented backfill can be explained by two factors. Firstly, referring to Figure 1, it can be seen that the dip span of the longwall is approximately 175 m for installations A and B, while the spans typically associated with the higher stress figures quoted are 200 m. Secondly, the Ventersdorp Contact Reef does not have bedding planes as do other reefs. The above factors lead to less inelastic closure. The stress thus required to clamp the hangingwall is less.

From Figures 8-11 it can be seen that there is a significant difference between the closures inside the bag and the roadway closures. Despite the lower vertical stresses required to clamp the hangingwall, there is nevertheless a significant component of inelastic closure present.

Dip stress profiles show stress contours along the dip section of the bag at different strains. Each line represents the stresses along the dip section of the bag for a given strain. Equal strains do not occur at different stations at the same time. From Figures 12 and 13 it can be seen that for a given strain the stresses reach a peak near the middle of the bag, and a minimum at the edge of the backfill. This indicates a hard centre with softer edges in the backfill bag, as reported by Adams and Gürtunca (1990).

Further support of the above discussion can be obtained by comparing the stresses of stations 1 and 2 on the closure contours in Figures 10 and 11. Each contour reflects the actual closures and stresses on a given day along the dip section of the bag. The lines between stations 1 and 2 are either flat or inclined slightly. The difference in closure between stations 1 and 2 expressed as a strain is very small due to the high stoping widths. A comparison of the vertical stresses (these are supplied in brackets on the figures) shows that, for similar strains, the stresses near the centre of the bag are significantly higher than near the edge. This indicates that the region in the middle of the bag is harder than the region near the edge of the bag (which agrees with the work of Fry and Hustrulid, 1990), and that there is a stress drop off near the edge of the bag due to dilation.

Figures 23 and 24 show that for both installations A and B, the vertical stresses at the stations near the edge of the bag (stations A1 and B1 respectively) are lower than those for the stations nearer the middle of the bag. This is true with respect to time (Figure 23) and strain (Figure 24). This shows that the effect of edge dilation occurs in real time as well as when one considers constant strain (Figures 12 and 13).

The average stoping width at installation C was 2,34 m, compared to 3,82 m and 3,61 m for installations A and B. This implies that any given closure at installation C will produce a higher strain, and consequently a higher stress in the backfill. This explains the higher stress values for installation C in Figures 23 and 24.

The stress curve for station C1 in Figure 23 is not lower than that for C3, as would be expected from the pattern for installations A and B. This may be because station C1 is on the fully confined side of the transition point.

Station C1 is 3,5 m from the edge of the bag, at a stoping width of 2,39 m. Station C1 was thus placed at a depth from the edge of the bag almost 1,5 times greater than the stoping width. Station A1 was placed at a depth 32 per cent greater than the stoping width, while station B1 was placed at a depth equal to the stoping width. Stations A1 and B1 were affected by dilation, while station C1 was not. This suggests that the depth of influence of the dilation along dip may be equal to one to 1,5 times the stoping width.

In the work by Adams et al (1991), it was proposed that there is transition point near the edge of a backfill bag. The vertical stress very near to the edge of the bag is near zero. The stress increases sharply along the dip section of the bag, to reach a maximum at the transition point. After the transition point, the stress plateaus with a slight dip towards the centre of the backfill (along dip). The sharp difference in behaviour between the backfill on either side of the transition point is due to dilation. The transition point thus marks the point at which the effect of dilation becomes negligible.

The 3,5 per cent strain line in Figure 12 increases sharply for station A3. This is probably due to a malfunctioning of the closure meter. It can be seen in Figure 8 that the closure curves for stations A1 and A2 start more rapidly than that of station A3. This may have been due to the closure meter at station A3 initially registering only a part of the total closure, and subsequently registering the full closure increments. This is supported by the constant gap between the closure lines for station A3 and the other stations. The constant closure difference would result in stresses being associated with lower strains, or conversely, the stress for any given strain is too high. Following this argument, all the stress contours in Figure 12 could be adjusted downwards at station A3. For example, the stress corresponding to 3,5 per cent strain for station A3 could be adjusted to approximately 1,3 MPa. This would produce a series of contours more similar to those of Figure 13.

5.3 Laboratory Behaviour

The results of the first test show the typical cemented backfill response of a stress drop followed by a stress build up. Typically, the stress drop occurs at a vertical stress of 1 MPa. Due to a higher horizontal to vertical aspect ratio, this occurred at a vertical stress of 2,5 MPa in the test.

For the second test, it was mentioned previously that the dilation was 20 per cent in the direction confined by geotextile fabric. This amount of dilation is unrealistic in terms of in situ conditions. When the material started to dilate under load, it moved out from under the loading platens because the loading platens above the sample were of the same dimensions as the sample. The dilation was thus much greater than in situ because of a lack of friction between the backfill and the platens.

From a comparison between Figures 15 and 17 it can be seen that confinement is necessary for cemented backfill to generate continually increasing vertical stresses as strain increases. At full confinement in the one direction and semi-confinement in the other, the vertical stresses are generated in an increasingly stiff stress strain curve. The effect of a lack of full confinement is shown in the curve for station D in Figure 17.

The confined compression behaviour is evident from Figure 18, in which significant horizontal stresses are generated. This behaviour is more clearly shown in Figures 19 and 20, where it can be seen that confined compression behaviour (Gürtunca et al., 1989) is reached at about 15 per cent strain in both the strike and dip (confined and semi-confined) directions. This shows that the sample becomes fully confined in both directions at the same time. The similar Ko values for both directions shows that the confinement conditions were similar in both directions, even though there was a 20 per cent dilation in the semi-confined direction. This indicates that the influence of the dilation was not felt near the centre of the sample. It was mentioned previously that there was a definite region of softness in a 200 mm band at the semi-confined edges, with the region inside this band being distinctly harder. This is borne out by the results of station D, compared to the results of stations A and C. The dilation thus affected the confinement conditions to a depth of 200 mm into the sample. This is the same length as the sample height.

The K ratios for station D are higher in the confined direction than the semi-confined direction (Figures 19 and 20), because for a constant vertical stress (Figure 17), the confined horizontal stress was able to increase while the semi-confined horizontal stress was constant.

The final load was 17,15 MN, at which the vertical stresses at the stations near the middle of the sample were over 30 MPa (stations A and C), while the vertical stress at station D was 2,22 MPa. Considering that the area of the sample was 1 m^2, it is apparent that the area in the middle of the sample took most of the load. This indicates that the central core of the material was stronger than the edges. This transfer of load from the softer edges to the harder core was reported by Fry and Hustrulid (1990).

The vertical stresses (Figure 17) started picking up at three to four per cent strain, even though the loading press was applying significant loads (at three per cent strain, the load was 0,72 MN). This is contrary to what would be expected from a cemented material. A possible explanation is that the load bearing surface was not perfectly flat, or not parallel to the loading platen. The surface may also have had local humps that served as stress concentrators, which prevented the load from influencing the stress meters until the humps had been levelled.

5.4 Comparison between In Situ and Laboratory Behaviour

The range of the in situ Ko value was 0,09 to 0,44, while the range of the laboratory Ko value was 0,42 to 0,58 (disregarding station D). The in situ Ko conditions were attained below five per cent strain, while Ko conditions were attained at 15 per cent strain in the confined laboratory test.

The softening of the edges with a harder interior occurred in the in situ backfill and in the test, as seen in Figures 10, 11 and 17 and discussed above.

The laboratory results confirmed that cemented backfill has the potential to achieve high stresses and strains in situ, even though the in situ strains have progressed slowly with time.

The simultaneous attainment of Ko conditions in the two horizontal directions in the laboratory test is similar to the banding of the in situ Ko values in that the confinement conditions at a particular point are similar in both directions.

The in situ results led to a suggested link between the stoping width and the depth of influence of dilation. The laboratory test results showed the influence of dilation

to be equal to the height of the sample, providing some experimental agreement with this suggestion.

5.5 Comparison Between In Situ and Elastic Closures

The results from installation A (Figure 21) show that a realistic in situ modulus for the hangingwall strata is 50 GPa, with parts of the in situ curve approaching the 60 GPa curve at relatively early stages. The initial in situ closure curve is higher than the 45 GPa curve, indicating a large component of inelastic closure.

The value of in situ modulus obtained from installation C (Figure 22) is 45 GPa. Similarly to installation A, the in situ curve approaches the 50 GPa curve at relatively early stages, with the initial in situ closure being above the 40 GPa curve.

As mentioned previously, the closure increments from station C1 (near the edge of the bag) were used for the in situ closure curve in Figure 22. The in situ closure profile for installation C (Figure 22) thus has a greater inelastic component than the profile used for installation A (Figure 21). This explains the lower overall figures for in situ modulus for installation C.

These in situ modulus figures compare well with figures quoted by Gürtunca and Adams (1991) and McKinnon (1989), who found that a suitable figure for in situ rockmass modulus was 52 GPa.

These results show that the closure of the VCR hangingwall is significant. A possible reason why the VCR has previously been thought to have low closure rates may be that much of the previous mining in the VCR has been more scattered. The associated smaller spans (compared to longwall applications) lead to less fracturing of the hangingwall. This and the lack of bedding planes in the hangingwall result in less inelastic closure.

As mentioned previously, the span of the 49 East longwall at WDL South Mine is less than a typical longwall span. The lower in situ closures when compared to other mines are thus expected. Yet the MINSIM-D results show that, for the smaller span, the closure is significant, and that it is more than is predicted by elastic theory.

Comparing the bag closures for installations A and B in Figures 8 and 9, the initial closures for installation A are much steeper than for installation B. There is initially a relatively small amount of similar closure before differential closure starts at installation B, compared to installation A. It is probable that the initial rapid closure was not recorded at installation B. The MINSIM-D modelling of installation B could not be compared to the in situ results for this reason.

5.6 Support Benefits of Cemented Backfill

The previous discussions have shown that cemented backfill fulfils the required support characteristics in that the backfill sustains stress and provides resistance to closure both on a local and regional scale.

In Figure 25, the stress strain curves for three types of support are plotted for comparison purposes. The in situ cemented backfill stress strain behaviour is plotted as a range between the results for stations B2 and C1. A laboratory curve of a confined compression test on deslimed tailings has been plotted as an example of uncemented backfill, while the pack load cell curve is from a pack in the same panel as the cemented backfill.

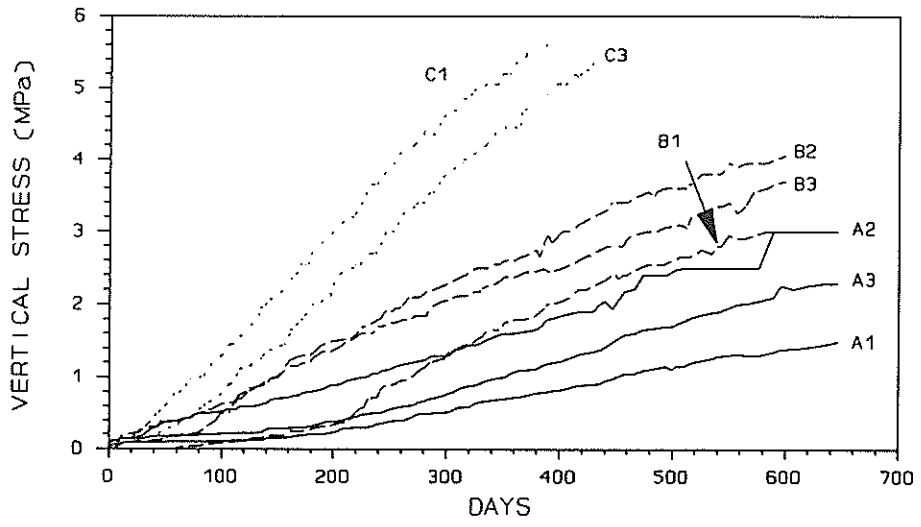

Fig. 23 - Vertical stresses for all three installations

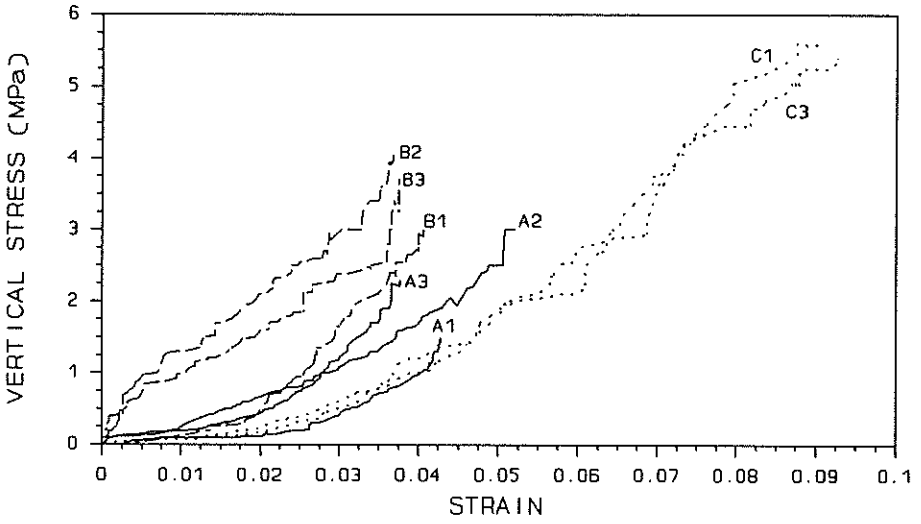

Fig. 24 - Composite stress strain graphs for all three installations

From the figure it can be seen that the pack has an initial stiffness similar to that of the cemented backfill. While the cemented backfill continues to provide resistance to closure, the pack yields and continues at the same stress. The cemented backfill thus provides resistance to closure after the pack has yielded. With backfill being installed on a regional basis, the benefits become enormous.

Uncemented backfill would slump excessively, and would not be able to support its own body weight in a stoping width of over 3,5 m. Typical figures of shrinkage are in the range 50-60 mm. Over a stoping width of 3,5 m, a shrinkage of 50 mm would amount to an unresisted closure of 1,4 per cent. The curve for the deslimed tailings is thus plotted at an offset of 0,014 on the strain axis.

Cemented backfill starts building up internal vertical stresses almost immediately, thus providing a resistance to closure much earlier than uncemented backfill. In effect, this means that the cemented backfill begins to perform its function as a support much earlier than uncemented backfill would do. As can be seen in Figure 25, the cemented backfill is also stiffer than uncemented backfill, which implies

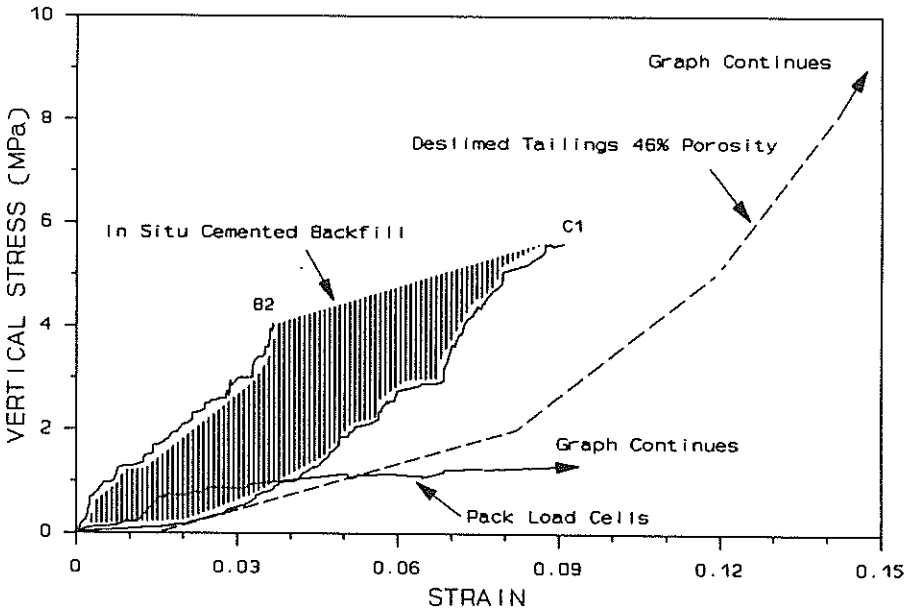

Fig. 25 - Comparison between the stress strain behaviour of cemented backfill,uncemented backfill and packs

that it is absorbing more energy early on.

6 CONCLUSIONS

The in situ confinement conditions in the backfill bag are similar in the dip and strike directions. This implies that the backfill is effectively confined in the dip direction, so that there is little or no lateral movement on dip except at the edge of the bag where dilation takes place.

The dilation has a significant influence to a limited depth from the edge of the bag. The in situ and laboratory results showed that there is a transition point between the zone where dilation has an influence and where it does not. This also defines the zones of partial and confined compression. There is some evidence to show that the extent of the zone of dilation is linked to the stoping width.

Clamping of the hangingwall occurs at vertical stresses of below 2 MPa, which is lower than the stresses reported for quartzite hangingwalls. This is because there is less inelastic closure in the VCR hangingwall due to smaller dip spans and the lack of bedding planes in the VCR.

There is nevertheless a significant component of inelastic closure present at WDL. The MINSIM-D elastic modelling showed that the in situ modulus is in the range 45-50 GPa.

The general behaviour of cemented backfill is qualitatively the same as uncemented backfill in that

- closure rates are reduced by the cemented backfill
- there is a stress drop off near the edges of the backfill
- the backfill clamps the hangingwall.

The overall three dimensional model as proposed by Adams et al. (1991) is supported by the in situ results.

In the high stoping width application, cemented backfill performs better than uncemented backfill because it provides an almost immediate and stiffer resistance to closure with little or no shrinkage. The cemented backfill is also able to support its own body weight, which avoids excessive dilation at the edge of the bag. Packs reach a yield point, whereas the cemented backfill sustains increasing loads.

7 ACKNOWLEDGEMENTS

The work in this report forms part of the Regional Support research program of COMRO. The co-operation of Management and Staff at Western Deep Levels, Ltd. is gratefully acknowledged.

8 REFERENCES

1. ADAMS,D.J., GÜRTUNCA,R.G., 1990. An Assessment of the Rock Mechanics Benefits of Comminuted Waste Backfill at Western Deep Levels Gold Mine. COMRO Reference Report 3/91.

2. ADAMS,D.J., GÜRTUNCA,R.G. and SQUELCH,A.P., 1991. The Three-dimensional In Situ Behaviour of Backfill Materials. 7th Int. Cong. on Rock Mechanics, Aachen, Germany, ISRM.

3. FRY,M.F., HUSTRULID,W.A., 1990. Split Platen Results with Application to Backfill at Great Mining Depths. Int. Deep Mining Conf. : Technical Challenges in Deep Level Mining, Johannesburg, South Africa, SAIMM.

4. GÜRTUNCA,R.G., ADAMS, D.J., 1991. A Rock Engineering Monitoring Programme at West Driefontein Gold Mine. J.S. Afr. Inst. Min. Metall., Vol 91, No. 12, pp. 423-433.

5. GÜRTUNCA,R.G., ADAMS, D.J., 1991. Determination of the In Situ Modulus of the Rockmass by the use of Backfill Measurements. J.S. Afr. Inst. Min. Metall., Vol 91, No. 3, pp. 81-88.

6. GÜRTUNCA,R.G., JAGER,A.J., ADAMS, D.J. and GONLAG,M., 1989. The In Situ Behaviour of Backfill Materials and the Surrounding Rock Mass in South African Gold Mines. 4th Int. Symp. on Mining with Backfill, Ontario, Canada.

7. HOPKINS,P.H., BEAUDRY,M.S., 1989. An Evaluation of Binder Alternatives for Hydraulic Mill Tailings. 4th Int. Symp. on Mining with Backfill, Ontario, Canada.

8. LAMOS,A.W., CLARK,I.H., 1989. The Influence of Material Composition and Sample Geometry on the Strength of Cemented Backfill. 4th Int. Symp. on Mining with Backfill, Ontario, Canada.

9. McKINNON, S.D., 1989. Protection of Deep Vertical Shaft Systems. Ph.D Thesis, University of the Witwatersrand, Johannesburg.

10. QUESNEL,W.J.F., de RUITER,H., PERVIK,A., 1989. The Assessment of Cemented Rockfill for Regional and Local Support in a Rockburst Environment. 4th Int. Symp. on Mining with Backfill, Ontario, Canada.

11. SQUELCH,A.P., 1990. Results of a Backfill Monitoring Programme at Vaal Reefs 5 Shaft. COMRO Reference Report 24/90.

12. VILES,R.F., BOILY,M.S. and DAVIS,R.T.H., 1989. New Materials Technologies Applied in Mining with Backfill. 4th Int. Symp. on Mining with Backfill, Ontario, Canada.

13. WHYATT,J.K., BOARD,M.P. and WILLIAMS,T.J., 1989. Examination of the Support Potential of Cemented Fills for Rockburst Control. 4th Int. Symp. on Mining with Backfill, Ontario, Canada.

APPENDIX I

SUPPLEMENTARY GRAPHS

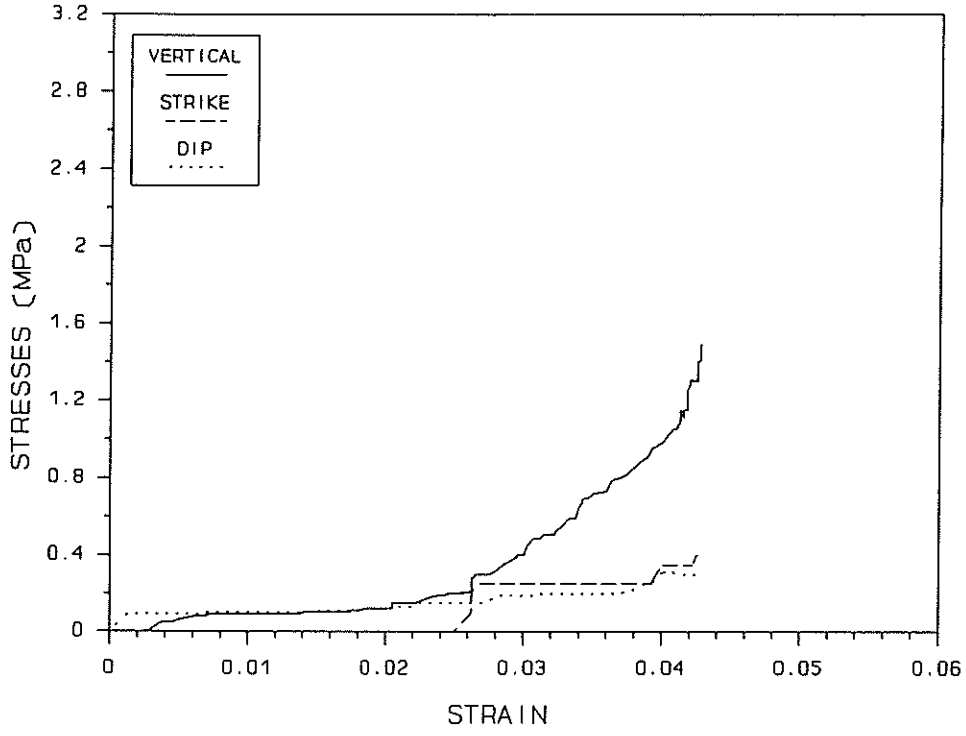

Fig. I1 - Stress strain behaviour at station A1

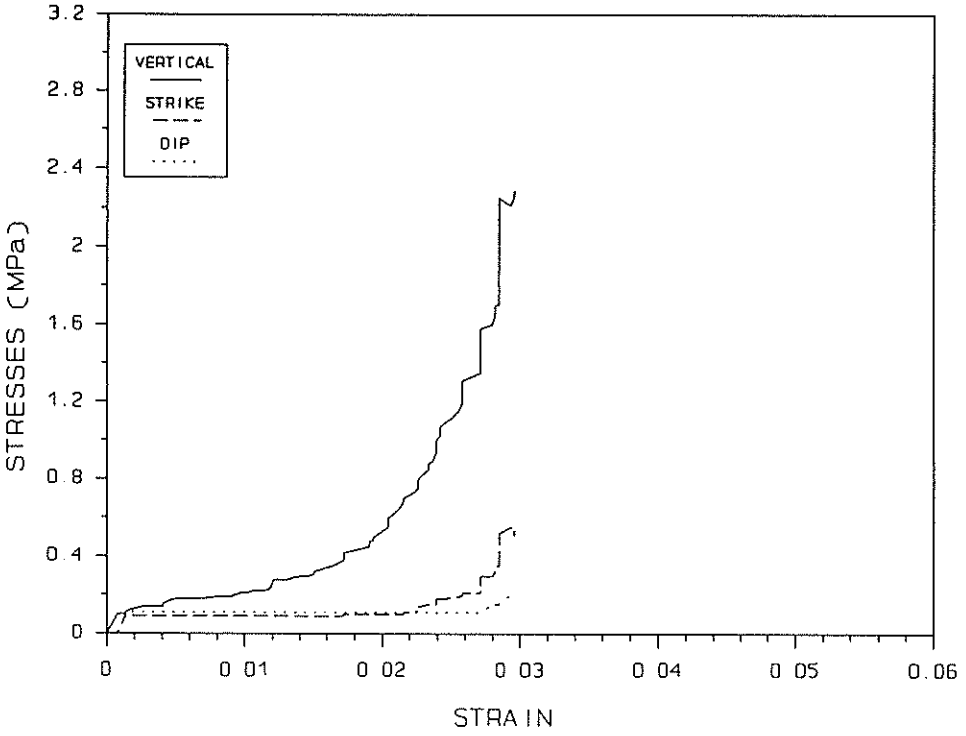

Fig. I2 - Stress strain behaviour at station A3

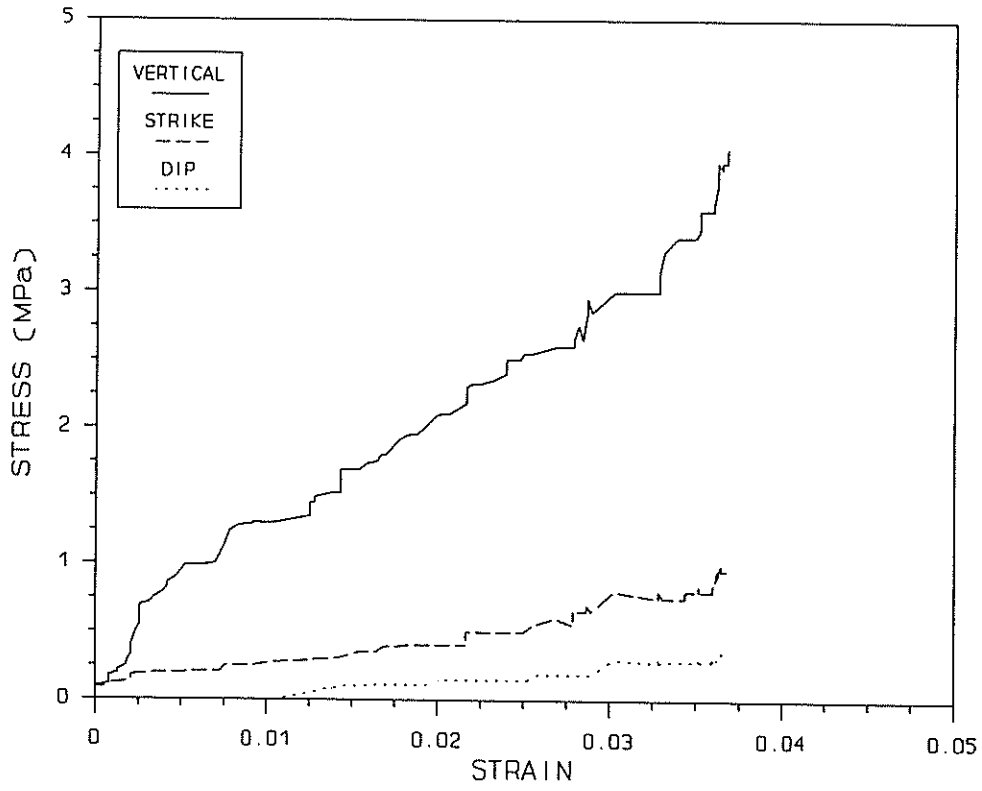

Fig. I3 - Stress strain behaviour at station B2

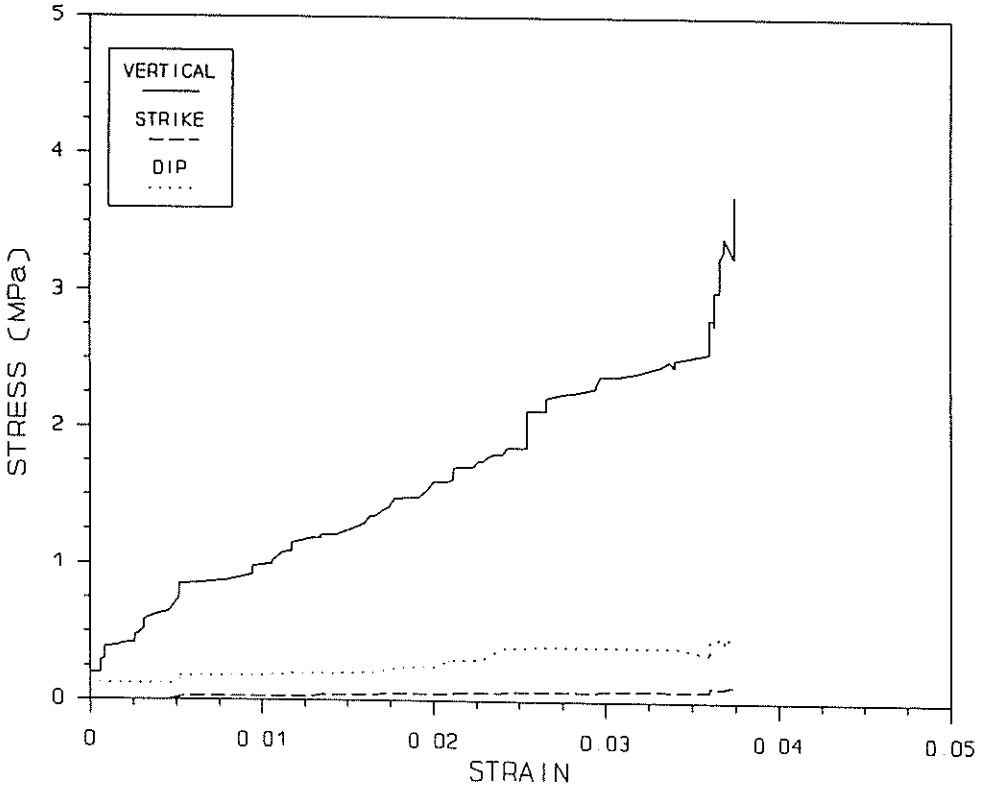

Fig. I4 - Stress strain behaviour at station B3

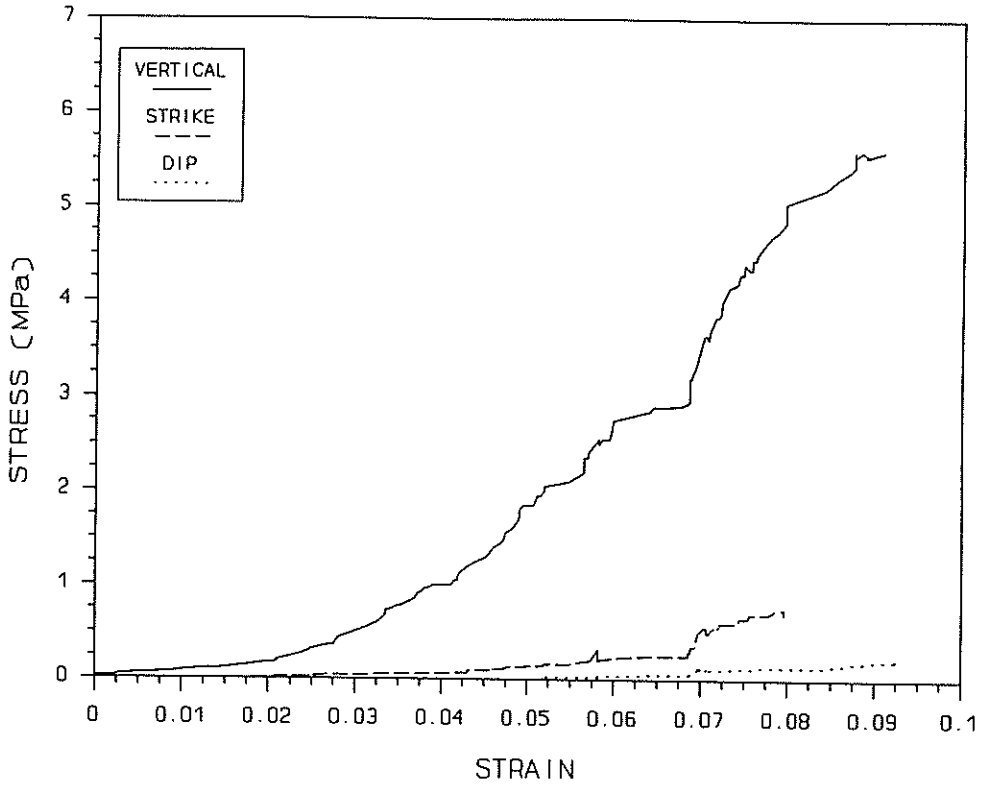

Fig. I5 - Stress strain behaviour at station C1

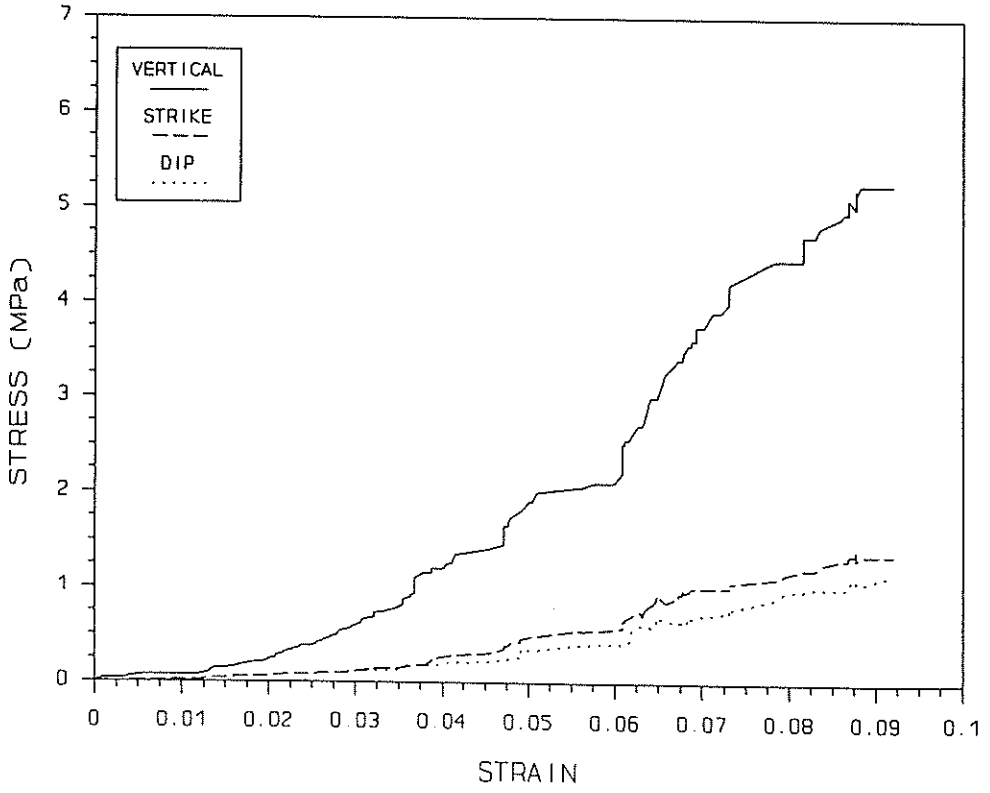

Fig. I6 - Stress strain behaviour at station C3